

Coherent nonlinear optics of quantum emitters in nanophotonic waveguides

Pierre Türschmann,^{1,2} Hanna Le Jeannic,³ Signe F. Simonsen,³ Harald R. Haakh,^{1,*}
Stephan Götzinger,^{4,5,1} Vahid Sandoghdar,^{1,4} Peter Lodahl,³ and Nir Rotenberg^{3,†}

¹*Max Planck Institute for the Science of Light, Staudtstr. 2, D-91058 Erlangen, Germany*

²*Linnwave GmbH, Henkestr. 91, D-91052 Erlangen, Germany*

³*Niels Bohr Institute and Center for Hybrid Quantum Networks,*

University of Copenhagen, Blegdamsvej 17, DK-2100 Copenhagen, Denmark

⁴*Department of Physics, Friedrich Alexander University Erlangen-Nürnberg (FAU), 91058 Erlangen, Germany*

⁵*Graduate School in Advanced Optical Technologies (SAOT), FAU, 91052 Erlangen, Germany*

(Dated: December 16, 2024)

Coherent quantum optics, where the interaction of a photon with an emitter does not scramble phase coherence, lies at the heart of many quantum optical effects and emerging technologies. Solid-state emitters coupled to nanophotonic waveguides are a promising platform for quantum devices, as this combination is scalable. Yet, reaching full coherence in these systems is challenging due to the dynamics of the solid-state environment of the emitters. Here, we review progress towards coherent light-matter interactions with solid-state quantum emitters coupled to nanophotonic waveguides. We first lay down the theoretical foundation for coherent and nonlinear light-matter interactions of a two-level system in a quasi-one-dimensional system, and then benchmark experimental realizations. We then discuss higher-order nonlinearities that arise due to the addition of photons of different frequencies, more complex energy-level schemes of the emitters, and the coupling of multiple emitters via a shared photonic mode. Throughout, we highlight protocols for applications and novel effects that are based on these coherent interactions, the steps taken towards their realization, and the challenges that remain to be overcome.

I. INTRODUCTION

Quantum optics has come a long way. We no longer focus solely on fundamental demonstrations of the quantum nature of atoms, photons or their interactions, but rather find ways to integrate these constituents into increasingly complex systems. These provide an ever-growing view of the rich realm of many-body quantum physics [1] and bring us closer to functional quantum technologies such as quantum networks [2–4] and, ultimately, quantum computers [5, 6].

One basic element that has the potential to fulfill many of the functionalities required in complex, and active, quantum architectures is a quantum emitter coupled to a photonic waveguide, as sketched in Fig. 1. Nanophotonic waveguides confine and guide light, reshape the emission from dipole sources to match their fundamental mode [7–9] and can be engineered to strongly suppress emission to free-space [10], resulting in efficient emitter-photon coupling [11]. An emitter efficiently coupled to a waveguide can therefore act as a source of high-quality single photons [12], for example for quantum information processing with linear optical systems [13, 14]. The strong confinement of light in waveguides also leads to the presence of a large longitudinal component of the electric field, and the interaction of this vector field with circular dipoles can result in unidirectional emission [15–18]. These directional light-matter interactions enable the creation of

chiral quantum optical elements such as optical isolators, single photon routers, quantum logic gates and even networks [19].

Spurred by this potential, researchers have, in the past few years, worked to couple a variety of quantum emitters to waveguides, including single organic molecules [20–23], a variety of colour centers in diamond [24–27], atoms [28–31], quantum dots [9] and superconducting qubits [32]. The latter colloquium specifically focuses on quantum optical nonlinearities in one-dimensional systems of superconducting qubits and Rydberg atoms, which are not covered in the current Review.

The challenge to interfacing solid-state emitters with nanophotonic waveguides is in keeping the ensuing light-matter interactions coherent. As sketched in Fig. 1a there are many possible sources of noise in solid-state systems, from ballistic or trapped charges near the emitter, to spin noise in the surrounding nuclear bath, to the coupling to phonons or to vibration in the vicinity of the emitter [33–36]. The methods implemented to overcome these processes depend on the type of quantum emitter and include, for example, the careful crystallization of the host matrix of single organic molecules [20, 37], embedding epitaxially grown quantum dots in a diode to shield them from electronic fluctuations [38, 39], using Purcell enhancement to overcome dephasing [24, 40, 41] and searching for better shielded defects within diamond [42].

Here, we review the current state-of-the-art in coherent quantum optics in waveguides, focusing on quantum optical nonlinearities. We begin with the theoretical background that describes coherent quantum optics of two-level systems in one dimension, highlighting the important parameters and figures of merits associated

* Current address: Federal Ministry of Education and Research, D-53170 Bonn, Germany

† Email: nir.rotenberg@nbi.ku.dk

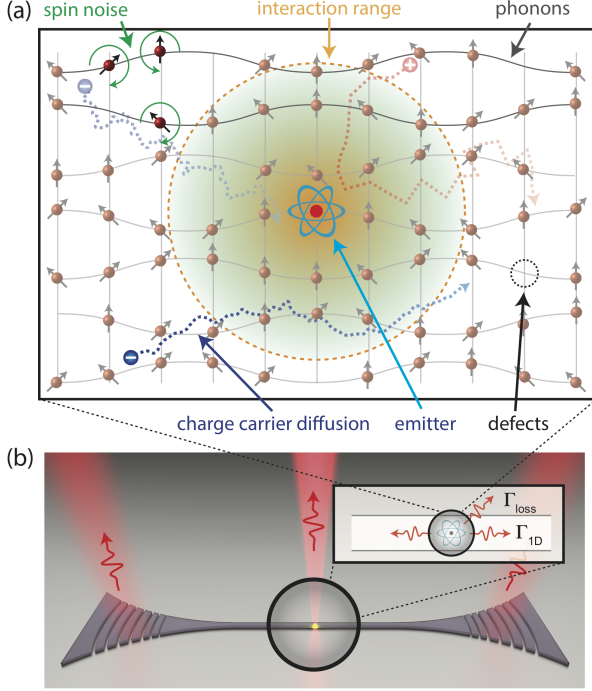


FIG. 1. The basic system considered within this review: a quantum emitter coupled to a quasi-one-dimensional photonic waveguide. The coherence of this quantum system is degraded by the interaction of the emitter with the solid-state environment, as discussed in the text. (a) Here, sources of noise such as charge, spin, phonons and nearby defects are schematically depicted. (b) Emission, in this system, occurs either into the guided modes, with a rate Γ_{1D} , or is lost into other modes with a rate Γ_{loss} .

with these interactions and the corresponding experimental demonstrations. We then review higher-order quantum optical nonlinearities, touching on effects that require multiple photons and extending beyond two-level systems, before concluding with a discussion of coherent quantum optics in multi-emitter systems.

II. NONLINEAR RESPONSE OF A TWO-LEVEL SYSTEM COUPLED TO A WAVEGUIDE

A. Transmission and reflection

Of the many theories developed to describe quantum light-matter interactions [43] the Green's function formalism is particularly well suited to describe the coherent interaction of guided photons with two-level systems (TLSs) [44]. This formalism allows for a full quantum treatment of dispersive and absorbing open systems and therefore spans both plasmonic and dielectric waveguides and, importantly, can be extended to multi-emitter systems (Sec. IV). In this section, we briefly outline this formalism, focusing on measurable signatures of coherent

light-matter interactions with TLSs embedded in one-dimensional waveguides.

The Hamiltonian describing the interaction of a TLS with light in a single photonic mode, in a reference frame rotating at the angular frequency of the light field ω_P , is

$$\hat{\mathcal{H}} = -\hbar\Delta_P\hat{\sigma}_{eg}\hat{\sigma}_{ge} + \hbar\omega_P\hat{\mathbf{f}}^\dagger(\mathbf{r})\hat{\mathbf{f}}(\mathbf{r}) - \hat{\mathbf{d}} \cdot \hat{\mathbf{E}}(\mathbf{r}), \quad (1)$$

where $\Delta_P = \omega_P - \omega_A$. The first term describes the TLS, whose transition energy is $\hbar\omega_A$ and whose coherences between the i and j levels are given by $\hat{\sigma}_{ij} = |i\rangle\langle j|$. Likewise, the second term relates to the excitation of the light field, here taken to have energy $\hbar\omega_P$, described by the creation and annihilation bosonic operators $\hat{\mathbf{f}}$ and $\hat{\mathbf{f}}^\dagger$.

The last term of Eq. 1 describes the light-matter interaction, which is mediated by the transition dipole of the emitter. Here, the dipole operator can be written in terms of the dipole matrix elements $\mathbf{d} = \langle g|\hat{\mathbf{d}}|e\rangle$ as $\hat{\mathbf{d}} = \mathbf{d}^*\hat{\sigma}_{eg} + \mathbf{d}\hat{\sigma}_{ge}$ and $\hat{\mathbf{E}}(\mathbf{r})$ is the electric field operator, to which we will return shortly.

First, however, it is instructive to consider solely the state of the emitter, using the reduced density matrix for the TLS $\hat{\rho}$, which is related to the expectation values of the atomic operators through $\langle\hat{\sigma}_{ij}\rangle = \rho_{ji}$. The emitter density matrix operator evolves according to [45]

$$\frac{d\hat{\rho}}{dt} = -\frac{i}{\hbar}[\hat{\mathcal{H}}, \hat{\rho}] + \mathcal{L}[\hat{\rho}], \quad (2)$$

where the Lindblad operator for the single emitter system [46, 47]

$$\mathcal{L}[\hat{\rho}] = \sum_{ij} \frac{\Gamma_{ij}}{2} (2\hat{\sigma}_{ji}\hat{\rho}\hat{\sigma}_{ij} - \hat{\sigma}_{ii}\hat{\rho} - \hat{\rho}\hat{\sigma}_{ii}) \quad (3)$$

accounts for both the decay and decoherence of the emitter. For the emitter-waveguide system, this operator has three non-zero terms: $\Gamma_{eg} \equiv \Gamma$ which is the spontaneous emission rate associated with the transition from $|e\rangle$ to $|g\rangle$ and $\Gamma_{ee} = \Gamma_{gg} \equiv \Gamma_{\text{deph}}$ which is the pure dephasing of the system through which it decoheres without undergoing a transition.

Equation 2 can be solved using the rotating wave approximation and by assuming Markovian dephasing processes to yield the steady-state ($\frac{d}{dt}\hat{\rho} = 0$) elements of the reduced density matrix,

$$\rho_{ee} = \frac{2\Gamma_2\Omega_P^2}{\Gamma(\Gamma_2^2 + \Delta_P^2 + 4(\Gamma_2/\Gamma)\Omega_P^2)}, \quad (4)$$

$$\rho_{ge} = -\frac{\Omega_P(i\Gamma_2 + \Delta_P)}{\Gamma_2^2 + \Delta_P^2 + 4(\Gamma_2/\Gamma)\Omega_P^2}, \quad (5)$$

where $\Gamma_2 = \Gamma/2 + \Gamma_{\text{deph}}$ and we have defined the Rabi frequency to be $\Omega_P = \mathbf{d} \cdot \mathbf{E}/\hbar$ for the driving field amplitude at the position of the emitter $\mathbf{E} = \langle\hat{\mathbf{E}}\rangle$. Note that the other two elements of the reduced density matrix are simply $\rho_{gg} = 1 - \rho_{ee}$ and $\rho_{eg} = \rho_{ge}^*$. Interestingly, Eq. 4

describes the spontaneous emission of the emitter, showing both the amplitude saturation and linewidth broadening as a function of Ω_P .

To understand how the emitter interacts with photons propagating through the waveguide we return to Eq. 1, now writing the electric field operator as $\hat{\mathbf{E}}(\mathbf{r}) = \hat{\mathbf{E}}^+(\mathbf{r}) + \hat{\mathbf{E}}^-(\mathbf{r})$, where in general [48]

$$\hat{\mathbf{E}}^+(\mathbf{r}, \omega) = i\mu_0 \sqrt{\frac{\hbar}{\pi\epsilon_0}} \frac{\omega^2}{c^2} \int d\mathbf{r}' \sqrt{\epsilon_I(\mathbf{r}', \omega)} \mathbf{G}(\mathbf{r}, \mathbf{r}', \omega) \cdot \hat{\mathbf{f}}(\mathbf{r}', \omega). \quad (6)$$

Here, we explicitly note the frequency dependence of the different quantities (that, henceforth, will be removed for clarity and understood to be evaluated at ω_P). The presence of the imaginary component of the dielectric function ϵ_I along side $\hat{\mathbf{f}}$, as required by the fluctuation dissipation theorem [49], ensure that this formalism is valid for dispersive and absorbing systems. Intuitively, this equation states that the field at any position \mathbf{r} is comprised of photons emitted at all positions \mathbf{r}' that then propagate back to \mathbf{r} . This process is described by the Green's tensor $\mathbf{G}(\mathbf{r}, \mathbf{r}', \omega)$, meaning that photons propagate through the system in the same manner as classical electromagnetic waves.

The dipole projected Green's function for a one-dimensional waveguide is [50, 51]

$$\begin{aligned} \mathbf{g}(\mathbf{r}_i, \mathbf{r}_j) &= \frac{\mu_0 \omega_A^2}{\hbar} \mathbf{d}^*(\mathbf{r}_i) \cdot \mathbf{G}(\mathbf{r}_i, \mathbf{r}_j) \cdot \mathbf{d}(\mathbf{r}_j), \\ &= i \frac{\beta \Gamma}{2} e^{ik_P |z_i - z_j|}, \end{aligned} \quad (7)$$

where k_P is the wavenumber of the photonic mode and the ratio of photons emitted into the waveguide mode to the total emission is $\beta = \Gamma_{1D}/\Gamma$. Following some algebra, this equation for $\mathbf{g}(\mathbf{r}_i, \mathbf{r}_j)$ allows us to rewrite Eq. 6 in terms of the incident $\hat{\mathbf{E}}_P^+$ and scattered fields

$$\hat{\mathbf{E}}^+(\mathbf{r}) = \hat{\mathbf{E}}_P^+(\mathbf{r}) + i \frac{\beta \Gamma}{2\Omega_P} \hat{\mathbf{E}}_P^+(\mathbf{r}) \hat{\sigma}_{ge}. \quad (8)$$

Equations 4, 5 and 8 allow us to quantify the light-matter interaction of the TLS with guided photons. The transmission through the waveguide, for example, is $T = \langle \hat{\mathbf{E}}^- \hat{\mathbf{E}}^+ \rangle / \langle \hat{\mathbf{E}}_P^- \hat{\mathbf{E}}_P^+ \rangle$, which can be written using Eq. 8 as

$$T = 1 + \left(\frac{\beta \Gamma}{2\Omega_P} \right)^2 \rho_{ee} + i \frac{\beta \Gamma}{2\Omega_P} (\rho_{eg} - \rho_{ge}). \quad (9)$$

The first term of this equation, which depends on the population of the excited state of the emitter, is typically thought to govern the incoherent interactions, while the second term depends on the atomic coherences and is therefore viewed as the source of the coherent interactions. This view is particularly attractive since $\langle \hat{\sigma}_{ee} \rangle$ dominates over $\langle \hat{\sigma}_{eg} \rangle$ at high energies (c.f. Eqs. 4 and 5).

In light of these equations and the prefactors of Eq. 9, however, it is clear that both terms have the same power dependence, and it is not so simple to separate the coherent and incoherent contributions to the transmitted field.

Such a separation is, however, relatively straight forward in the low power and no detuning limit, where we can use Eqs. 4 and 5 to rewrite the transmission as,

$$T \approx 1 - \frac{\Gamma}{\Gamma_2} \beta + \frac{\Gamma}{2\Gamma_2} \beta^2, \quad (10)$$

where it is clear that in the limit of no pure dephasing all terms contribute. If we then define the fraction of coherent interactions to be $\beta_{co} \equiv \Gamma_{1D}/2\Gamma_2$, we can rewrite the low-power transmittance as,

$$T \approx (1 - \beta_{co})^2 + \beta_{co} (\beta - \beta_{co}), \quad (11)$$

where the first and second terms are the coherent and incoherent contributions.

More generally, the transmission expressed in terms of the system parameters is

$$T = 1 - \frac{\beta \Gamma \Gamma_2 (2 - \beta)}{2(\Gamma_2^2 + \Delta_P^2 + 4(\Gamma_2/\Gamma) \Omega_P^2)}. \quad (12)$$

Similarly, the reflection from the TLS is

$$R = \frac{\beta^2 \Gamma \Gamma_2}{2(\Gamma_2^2 + \Delta_P^2 + 4(\Gamma_2/\Gamma) \Omega_P^2)}, \quad (13)$$

and the losses due to the scattering of light out of the waveguide mode is simply $S = 1 - T - R$. Note that these equations have been derived for excitation by a weak, continuous wave beam, but also hold for spectrally narrow single photons.

A clear signature of the coherent interaction between a TLS and an emitter can be found in the transmission (and reflection) signals [53]. For a perfect system ($\beta \rightarrow 1$, $\Gamma_{\text{deph}} \rightarrow 0$) in the low-power limit ($\Omega_P \rightarrow 0$) all single-photons are reflected, leading to a perfect extinction of the transmission $\Delta T = T(\Delta_P = \pm\infty) - T(\Delta_P = 0) = 1$. As is evident from Eq. 12, this extinction nonlinearly depends on the power, coupling efficiency and dephasing rate of the emitter. A perfect extinction is not possible with tightly focused plane-waves, where a theoretical maximum of $\Delta T = 0.85$ has been calculated [54]. Rather, perfect extinction in free-space requires perfectly matching the dipole mode with the excitation beam, a notoriously difficult proposition that motivates the importance of nanophotonic platforms. Waveguides, as we noted earlier, both reshape the radiation pattern of dipoles to match their fundamental modes [7, 8] and are non-diffracting, meaning that these structures are particularly well suited to ideally interface with quantum emitters.

Coherent extinction has recently been observed in a variety of systems, as summarized in Fig. 2 and Tab. I. Multiple organic molecules have been coupled coherently

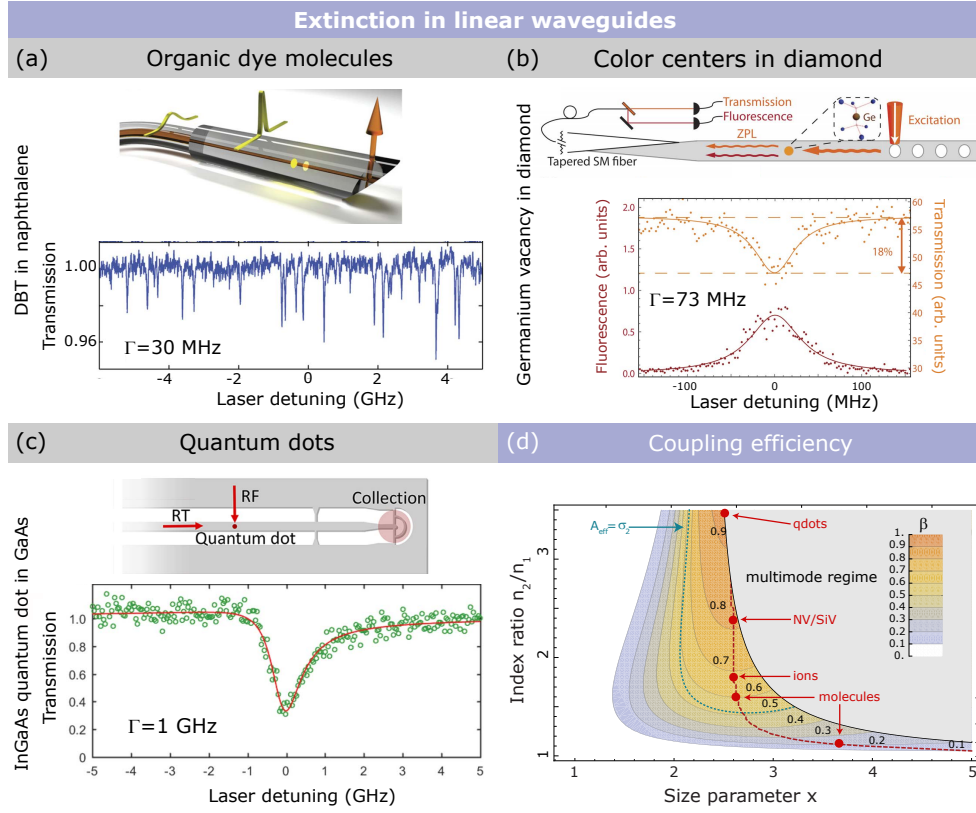


FIG. 2. State-of-the-art coherent extinction with a variety of solid-state quantum emitters in differing nanoguide geometries, including (a) single organic molecules, (b) Ge defects in diamond and (c) InAs quantum dots. Adapted from [20], [26] and [52], respectively. (d) Maximum achievable coupling coefficient β for cylindrical nanoguides of different core-sizes and core-surrounding refractive index contrast. The core-size is parameterized by the unitless variable $x = k_2 r$, where k_2 is the wavenumber of light in the bulk material of the core and r is the radius of the nanoguide. Achievable β -factors for the different solid-state quantum emitters are marked in red symbols (dashed red line denotes optimal achievable β for a given refractive index contrast), as is the geometry for which the effective mode area is equal to the scattering cross-section of an emitter (dashed blue line).

to a single nanoguide, each of which has a near-lifetime-limited transition that can be addressed individually through spectral-spatial selection [20] (Fig. 2a). Extinction up to $\Delta T \approx 0.09$ has been reported for this system [21]. Likewise, $\Delta T \approx 0.18$ has been measured for Ge vacancies, deterministically implanted in a diamond waveguide (Fig. 2b) [26], and $\Delta T \approx 0.67$ for InAs quantum dots embedded in a gated nanobeam waveguide [52] (Fig. 2c). In all cases, the limiting factor has been the β of the systems (c.f. Eq. 12). For nanoguides, such as those used in the aforementioned experiments, the maximally achievable β depends on the confinement of the guided mode that, in turn, is a function of the refractive index ratio between the waveguiding medium and its surrounding, and the geometrical size of the waveguide. These dependencies are plotted in Fig. 2d, where β is semi-analytically calculated for nanoguides with circular cross-sections [55], showing the largest possible β for the different quantum emitters.

Alternatively, β could be increased through the use of photonic resonators, or highly structured systems such as

photonic crystals. The generalization of Eqs. 12 and 13 to account for cavity Purcell enhancement is relatively straightforward and leads to the observation of Fano-like lineshapes in the transmission as the phase of the photons that do not interact with the emitter is now dependent on their spectral detuning from the resonance [57]. Coherent and deterministic light-matter interactions have, in fact, recently been demonstrated with a single molecule [58], defect centers [59] and quantum dots [60] in microcavities, where a $\Delta T \approx 0.99$ has been observed, albeit at a cost of operational bandwidth. Here, the emission into the photonic mode was Purcell enhanced, increasing the emission rate in the desired channel relative to other radiative channels and the dephasing rate. The nonlinear dependence of ΔT has been observed for both molecules [21] and quantum dots [52, 61, 62], where a critical flux of ≈ 1 photon per lifetime was found to saturate the emitter, as shown in Fig. 3a, since it can only scatter a single photon at a time. In a complimentary fashion, the phase of a scattered photon can be tuned, as the presence of a TLS fundamentally changes the re-

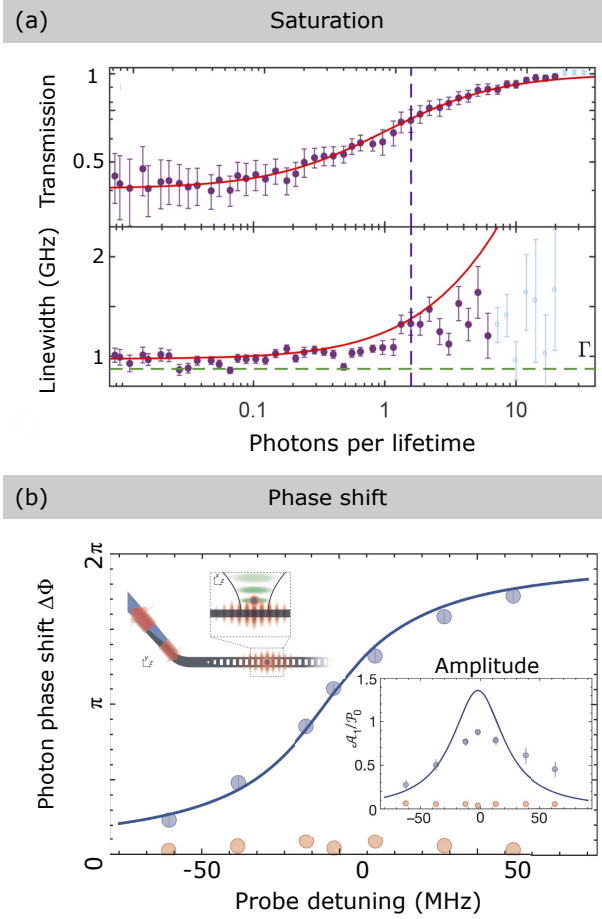


FIG. 3. (a) The coherent nonlinear response of a TLS is seen in the power-dependent extinction of the transmitted light, which vanishes as the photon flux increases beyond 1 photon per lifetime (top panel). As the same time, the bandwidth of the transition begins to power-broaden (bottom panel), signifying the loss of coherence in the light-matter interactions. Adapted from [52]. (b) An efficiently coupled TLS, here an atom evanescently coupled to a photonic crystal cavity (top inset), can also modulate the phase of the scattered photons. In fact, a markedly different response is shown in the presence of the emitter (blue symbols) and in its absence (yellow symbols). The bottom inset shows the corresponding, normalized count rate in one arm of an interferometer, relative to the expected cavity response (blue curve). Adapted from [56].

sponse of a nanophotonic system, as shown in Fig. 3b [56]. Altogether, these results hint at the power of coherent quantum optics in integrated photonic systems.

B. Nonlinearity and photon statistics

A more profound signature of the coherent nonlinearity of the TLS can be found in the ensuing photon statistics, which explicitly demonstrate the different response of the TLS to single and multiple incident photons. This

is seen in the normalized second-order correlation function,

$$g^{(2)}(\tau) = \frac{G^{(2)}(t, \tau)}{[G^{(1)}(t)]^2}, \quad (14)$$

where $G^{(1)}(t) = \langle \hat{\mathbf{E}}^-(t) \hat{\mathbf{E}}^+(t) \rangle$ and $G^{(2)}(t, \tau) = \langle \hat{\mathbf{E}}^-(t) \hat{\mathbf{E}}^-(t + \tau) \hat{\mathbf{E}}^+(t + \tau) \hat{\mathbf{E}}^+(t) \rangle$. The field operator used in these correlation functions is given in Eq. 8, but here $\hat{\sigma}_{ge}(t)$ evolves in time. For continuous wave excitation, the first-order correlation function can be simply derived by noting that in the steady-state $\rho_{ij} = \langle \hat{\sigma}_{ji}(0) \rangle$ and by using Eqs. 4 and 5. Similarly, the quantum regression theorem [45] allows us to express the two-time correlations found in $G^{(2)}(\tau)$ in terms of the steady state elements of the density matrix. In this manner, and in the low-excitation limit ($\Omega_P \rightarrow 0$), we can write

$$g^{(2)}(\tau) = 1 + \frac{\Gamma^2 \Gamma_2 \beta^4 e^{-\Gamma \tau} - \Gamma \beta^2 [2\Gamma_2 + \Gamma(\beta - 2)]^2 e^{-\Gamma_2 \tau}}{(\Gamma - \Gamma_2) [2\Gamma_2 + \Gamma\beta(\beta - 2)]^2}. \quad (15)$$

In the limit of no pure dephasing ($\Gamma_2 \rightarrow \Gamma/2$), this equation converges to that of Chang, *et al.*, [67].

The highly nonlinear response of a TLS is encoded into the photon statistics of the transmitted light. A signature of this nonlinearity is the photon bunching observed in $g^{(2)}(0)$, which we plot in Fig. 4a as a function of both β and the relative dephasing rate $\Gamma_{\text{deph}}/\Gamma$. The strong photon bunching is observed when $\beta \rightarrow 1$ and $\Gamma_{\text{deph}} \rightarrow 0$. Here, $g^{(2)}(0) \rightarrow \infty$, as $T \rightarrow 0$ (c.f. Sec. II A), meaning that all single-photon components of the incident coherent state are reflected. Conversely, in transmission, the coherent superposition of the zero and multi-photon components results in the photon bunching. This photon bunching has been observed with both QDs [61–63] and Ge vacancy centers [26] coupled to waveguides, with peak values of $g^{(2)}(0)$ ranging from 1.1 to 6. Higher values have recently been reported using a variety of emitters coupled to resonators, as summarized in Tab. I.

The physics underlying this multi-photon transmission was first considered by Shen and Fan who showed that it is comprised of two components: one in which the two photons are uncorrelated and therefore scatter independently, and one where the photons are correlated and cannot be considered independently [68, 69]. Shen and Fan derived analytic formulas for both components using a scattering matrix approach, and later using the input-output formalism [70]. Subsequently, Ramos and Garcia-Ripoll proposed an experimental method to measure the single and two photon scattering matrices using weak coherent beams [71].

A part of the correlated component of the two-photon wavepacket whose shape does not change due to scattering from the TLS exists. This component acts like a ‘quantum soliton’ and is known as a photon-photon

System	Extinction	Linewidth [†]	$g^2(0)$ [‡]	Details	Refs.
Organic molecules					
DBT-nanoguide	0.07 – 0.09	30(30) MHz	< 0.01	Observation of up to 5000 single-molecules coupled to the waveguide	[20], [21]
DBT- μ Cavity	0.99	40 (40) MHz	0.1 (21)	Measured $g^2(0)$ limited by timing-resolution of the detectors	[58]
InAs QDs					
QD-nanobeam	0.66	1.2(0.9) GHz	< 0.01	Charged stabilized and tunable by a diode	[12], [52]
QD-PhCW	0.07 – 0.35	1.1 – 4(0.9) GHz	< 0.01 (1.15)	Coherent nonlinearity at the single photon level	[61], [62]
QD-PhCW	0.85	1.36 (1.22) GHz	(6)	Charge stabilized and tunable by a diode	[63]
QD- μ Cavity	–	0.28 (0.28) GHz	(25 – 80)	Charge stabilized in a μ -pillar or μ -cavity	[64], [60]
Defect centers in diamond					
GeV-PhCW	0.18	73(26) MHz	< 0.08 (1.1)	Coherent nonlinearity at the single photon level	[26]
SiV-PhCW	0.38	590(90) MHz	< 0.15 (1.5)	Two emitters remotely entangled by Raman transitions	[24]
SiV-PhCC	> 0.95	4.6 GHz	0.23	Two Si vacancies, near-field coupled inside a single cavity	[59]
Atoms coupled to photonic waveguides					
Cs-nanoguide	0.01	5.8(5.8) MHz	-	More than 2000 resonantly coupled emitters	[28], [65]
Cs-PhCW	0.25	15(4.6) MHz	-	Mean number of coupled atoms is 3; observation of superradiance	[31]
Rb-nanoguide	0.20	6.1(6.1) MHz	-	1-6, mean number of coupled atoms; observation of superradiance	[66]
Rb-PhCC	-	53 MHz	0.12 (4.1)	Nanophotonic control of photon phase	[56]
[†] Natural linewidth, which may be Purcell enhanced, given in brackets.					
[‡] Bunching value observed in coherent transmission experiments given in brackets.					

TABLE I. State-of-the-art coherent light-matter interactions with solid-state quantum emitters coupled to nanophotonic waveguides. Atoms are included for completeness. PhCW: Photonic crystal waveguide; PhCC: photonic crystal cavity.

bound-state. This is much like photon-emitter bound-states, which are characterized by the entanglement between the light and matter degrees-of-freedom [72, 73], a hallmark of polaritonics [74]. The work on photonic bound-states was generalized to higher-number multiphoton bound states [75] and to their spectral and temporal signatures in structured photonic environments [76]. Experimental signatures of the correlated components of two [77] and three [78, 79] photon scattering events were recently reported with Rydberg atoms, but an unambiguous observation of a photonic bound-state is, to date, missing.

The highly nonlinear coherent scattering of guided photons from single emitters, and the ensuing strong correlations of photon-photon bound states, constitute a valuable quantum resource and have played a central role in recent proposals. The large disparity between the response of the emitter to single- and two-photon inputs can form the basis for a photon sorter, allowing for the realization of quantum nondemolition measurements [80], and for the creation of a Bell-State analyzer and controlled-sign gate [81]. This latter proposal may benefit from chiral coupling, meaning that all photons scatter in a single (forward) direction [19]. Interestingly, if this coupling is made asymmetric but not perfectly directional, then this passive two-level nonlinearity has

been predicted to act as a few-photon diode [82].

III. NONLINEARITIES OF MULTI-LEVEL SYSTEMS

In analogy to classical optics, there are a host of quantum optical nonlinearities beyond the interaction of photons with a two-level system described above. These higher-order quantum nonlinearities result from (i) the presence of multiple photons of different frequencies or (ii) a richer energy level structure of the emitter, and cannot be described by a perturbative susceptibility tensor like classical nonlinearities. In this section we describe these effects and highlight recent efforts to observe them in nanophotonic waveguides.

A. Dressed two-level systems

Two-level systems can coherently mediate the interaction between two different photons that, unlike the scenario described in Sec. II, can be frequency detuned. The resulting multiphoton nonlinear effects were first explored by Wu, Ezekiel, Duckloy and Mollow in 1977 who measured the transmission of a weak probe beam through

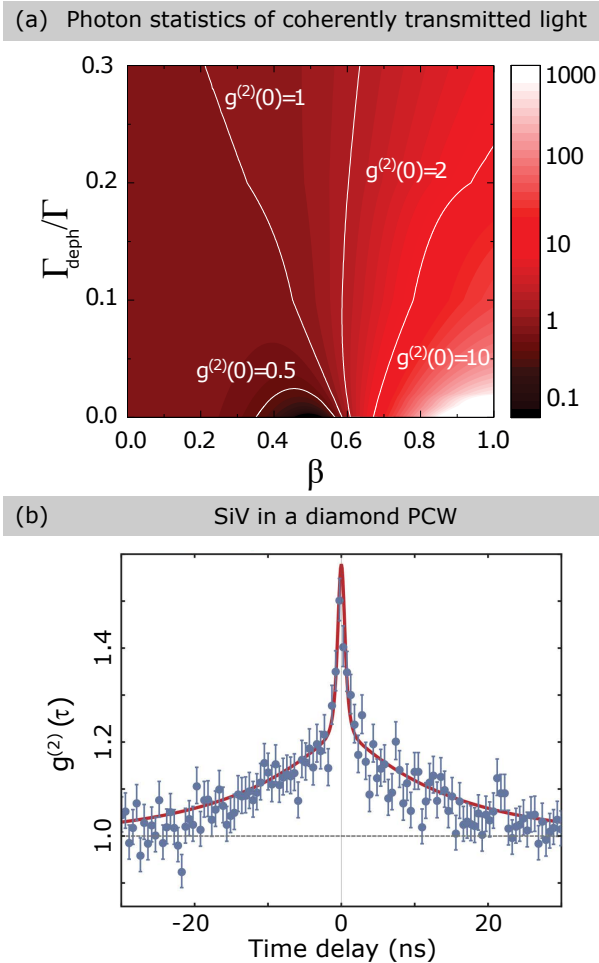


FIG. 4. Two-photon correlations for a weak coherent state scattering from a TLS embedded in a waveguide. (a) $g^{(2)}(0)$ as a function of both β and Γ_{deph} (Eq. 15), showing a strong photon bunching for well-coupled emitters with small pure dephasing. (b) Using an integrated nanophotonic waveguide-cavity coupled to a Si vacancy in diamond, researchers were able to observe a $g^{(2)}(0) \approx 1.5$. Adapted from [24].

a large ensemble of sodium atoms in the presence of a strong excitation laser [83]. Because of the weak light-matter interactions in these initial experiments, they were conducted using large ensembles of atoms and with intense control beams. In fact, 30 years would pass before technological progress enabled the observation of these nonlinearities at the single-photon single-emitter level, as we discuss below, when spectra such as those shown in the right panel of Fig. 5a where recorded using a single molecules [21, 84].

The physics underlying these spectra can be understood in terms of the three available transitions of the dressed state picture [85], where the bare states of the emitter hybridize with the manifold of light states, as shown in the left panel of Fig. 5a. First, the emitter resonance, which is observed as an extinction of the transmis-

sion as in Sec. II A, is AC-Stark shifted by the presence of pump photons (red arrows). Second, when the pump and signal are only slightly detuned, the emitter can mediate the transfer of photons between the two beams, which appears as a kink in the transmission spectra (corresponding to the green transition). Finally, a stimulated process that requires two pump photons can coherently amplify the signal beam without the need for population inversion, resulting in the bump of the transmission signal (corresponding to the blue transition). A theoretical model, based on the Optical Bloch Equations, accurately reproduces these complex spectra [86, 87].

Initially, observing these multicolour nonlinear effects with single emitters proved challenging, due to the low probability of each photon interacting with an emitter in bulk. These constraints were first overcome using a combination of sensitive lock-in techniques and ultra-strong pump fields, to observe the signatures of these nonlinearities at the 10^{-5} level, first in the absorption [88] and then the transmission [89] of a single quantum dot in a bulk medium. Maser *et al.* improved this signal by three orders of magnitude by focusing tightly on a single organic molecule with a transform-limited transition, embedded in a thin organic matrix. Using this same platform, researchers were then able to observe these multicolour nonlinearities mediated by a single organic molecule coupled to a waveguide on a photonic chip [21], as shown in Fig. 5b. Here, a clear nonlinear dependence of both the extinction and coherent amplification signals on the detuned pump photons is seen. Note, however, that even in this most recent experiment the extinction peaks at $\Delta T \approx 0.1$ due to a weak molecule-waveguide coupling of only $\beta = 0.08$. Regardless, this increased sensitivity both drastically reduced the amount of pump photons needed to observe these effects and allowed for the observation of additional nonlinear effects such as the four-wave-mixing shown in Fig. 5c [84].

Experimentally, the current challenge is to reach the regime where these multicolour nonlinearities can be deterministically observed, and perhaps exploited to control light-matter interactions at the single-photon level. This requires that the light-matter coupling efficiency approaches unity while maintaining a fully coherent interaction (i.e. $\Gamma_{\text{deph}} = 0$), further motivating the use of structured nanophotonic waveguides and resonators.

B. Three and four level emitters

Although we often approximate quantum emitters as TLS, they may actually have a much richer energy level structure that give rise to new coherent and nonlinear quantum optical effects. In recent years there have been many theoretical studies on the use of waveguides to enhance and exploit these effects, laying out the framework for future experiments.

A prototypical example of such a coherent, multi-level quantum optical nonlinearity is electromagnetically

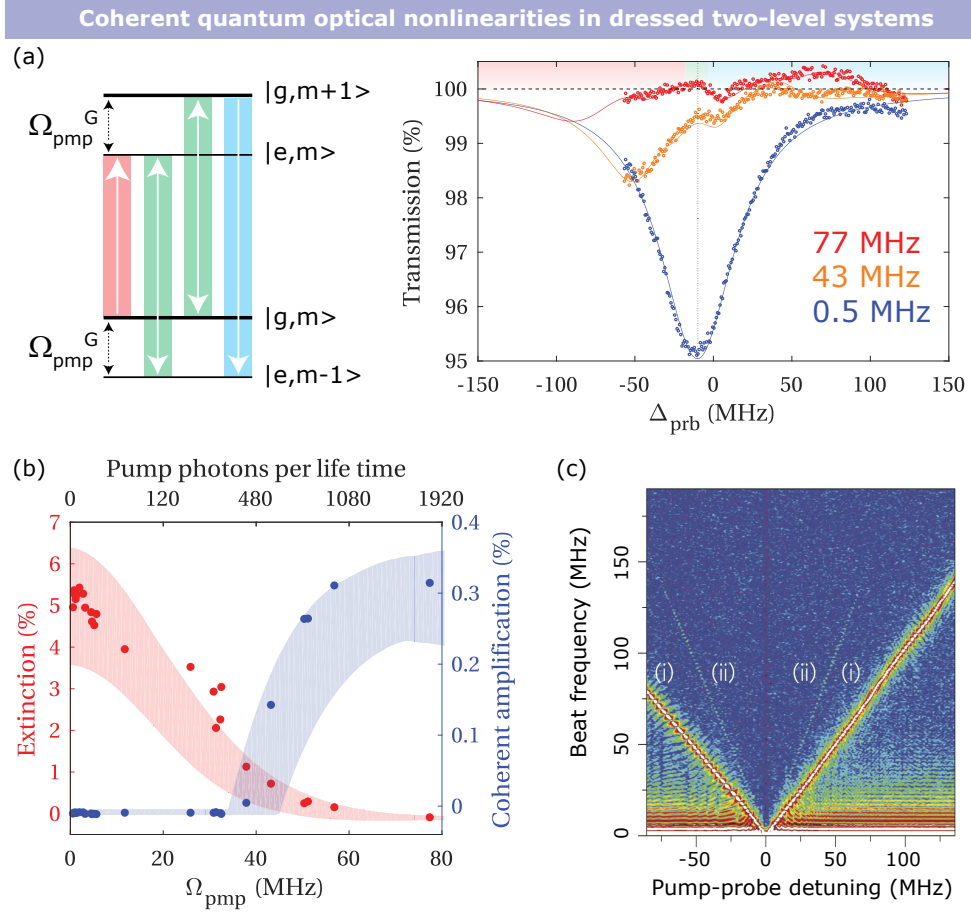


FIG. 5. Coherent quantum optical nonlinearities in dressed two-level systems. (a) The transmission spectra of photons scattering from a single organic molecule embedded in a nanoguide, evolves nonlinearly as a function of the strength of a control beam with Rabi frequency Ω_{pmp} [21]. The features of the red and orange curves can be understood in terms of the three available transitions between the states of the system, as shown to the left; each manifold of states is described by the state of the TLS and the photon number, here $|e\rangle$ or $|g\rangle$ and $|m\rangle$, respectively, and the level splitting is given by the generalized Rabi frequency $\Omega_{\text{pmp}}^G = \sqrt{\Delta_{\text{pmp}}^2 + \Omega_{\text{pmp}}^2}$. Here, a Stark-shift of the resonance (red), a coherent energy transfer between the signal and control photons (green), and a coherent amplification of the signal photons (blue) are observed. (b) The nonlinear dependence of the coherent extinction and amplification as a function of control beam strength. Adapted from [21]. (c) Four-wave-mixing observed using a single organic molecule as the nonlinear medium. This nonlinear signal manifests at twice the beat frequency (ii) as the scattered signal (i). Adapted from [84].

induced transparency (EIT). EIT occurs when, in the presence of a control field, destructive quantum interference between two transitions of a three-level system (c.f. Fig. 6a) prevents absorption of a weak signal field [90]. The coherent control of quantum absorption enables, for example, the storage and retrieval of quantum states, a crucial requirement for emergent quantum technologies [91]. In this, and other similar demonstrations, the low emitter-photon interaction probabilities necessitated the use of dense atomic ensembles, as was also the case when the atoms were weakly coupled to a waveguide [92–94]. Using waveguides to enhance the emitter-photon interaction can bring EIT to the single-photon and single-emitter level [95, 96], and such a system could form the

basis for a single-photon, all-optical switch [97].

Other coherent effects in three-level systems can be used to control the transport of photons. Population inversion of a single molecule, for example, allowed it to act as a quantum optical transistor [99, 100], coherently attenuating or amplifying a stream of photons. Interestingly, it is possible to form an optical transistor using a three-level Λ system without the need for population inversion. Rather, the coherent reflection and transmission outlined in Sec. II A can be used, in conjunction with a gate pulse that effectively couples or decouples the emitter from the waveguide, bringing the transistor to the single-photon level if the emitter is efficiently coupled to the photonic mode [67, 95] (c.f. Fig. 6b). Similarly,

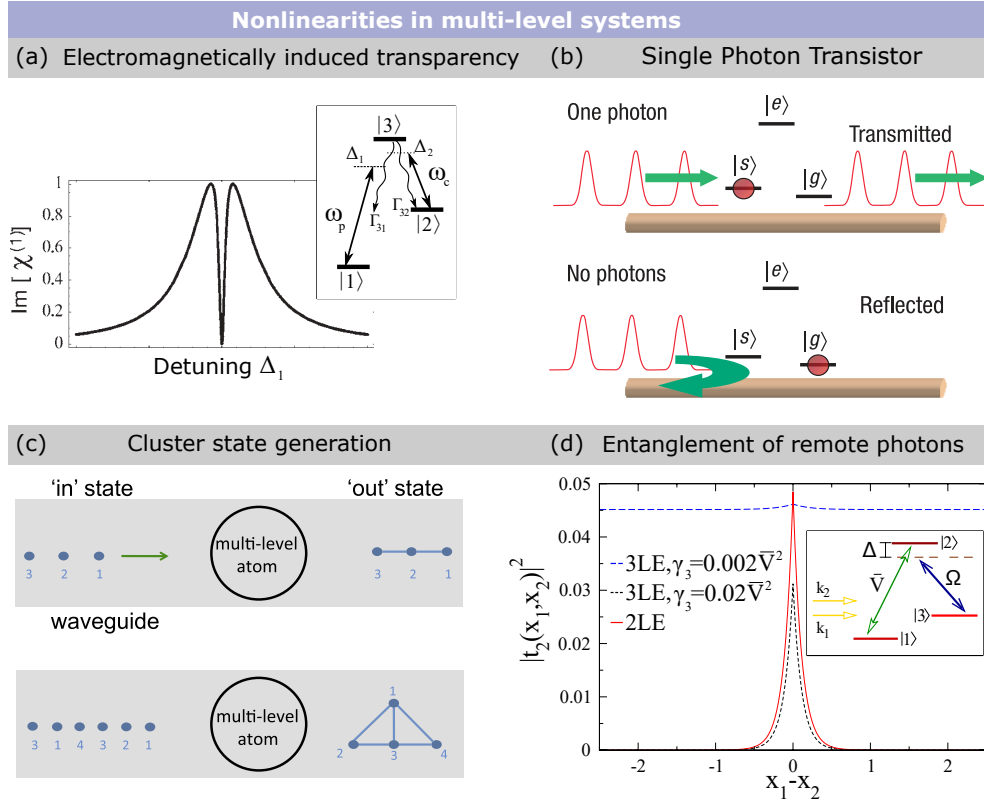


FIG. 6. (a) Generic Λ -type scheme (left) and spectrum (right) for EIT where a probe field of frequency ω_P and control field of frequency ω_C interact with a quantum emitter. In the presence of the control beam transition $|1\rangle \rightarrow |3\rangle$ is inaccessible and hence the absorption spectra sharply falls to 0 on resonance. Adapted from [90]. (b) Schematic diagram of a single-photon transistor based on a three-level emitter. The storage of a gate pulse containing zero or one photon conditionally spin-flips the state of the emitter, depending on the photon number. A subsequent incident signal field is then either transmitted or reflected depending on the state of the emitter. Adapted from [67]. (c) Example of photonic cluster state generation by sequential scattering from a multi-level emitter. In the top panel, three un-entangled photons sequentially scatter from an emitter, creating a three-photon matrix product state. In the bottom panel, four photons scatter from the emitter. After the fourth photon scatters, the first and third photons are re-scattered, creating a two-dimensional projected entangled pair state. Adapted from [98]. (d) Calculated two-photon spatial probability distribution after the scattering of two photons off a driven, three-level emitter (energy-level scheme shown in inset). In the low-loss limit (i.e. $\gamma_3 \approx 0$) the two-photon state is delocalized, providing a route to the creation of extended entangled states. As γ_3 increases, the behaviour of the driven system begins to resemble that of a two-level emitter. Adapted from [96].

control over the state of a ladder-type emitter coupled to a waveguide can switch, or even impart a π phase shift to a guided photon [101]. Theories of the interaction of few photons with three (or higher) level emitters predict the generation, or even engineering, of entangled photonic states. For example, two distinguishable photons can be entangled as they scatter from a ladder-type emitter, with the degree of entanglement depending on the spectral content of the photons [102]. The subsequent scattering of additional photons could thus be used to create large photonic entangled states, as shown in Fig. 6c. The controlled re-scattering of selected photon pairs from the entangled chain would create a photonic cluster state [98], which is a required resource in one-way quantum computing architectures [103].

Photonic bound states (c.f. Sec. II B) are also created

when few-photon coherent states scatter from multi-level emitters [104]. In contrast to the scattering from two-level emitters, the presence of additional levels provides a route to the controlled shaping of the bound state. Driving a resonance of a Λ -type emitter, for example, can delocalize the two-photon wavepacket formed as the pair of photons scatter from the second transition (Fig. 6d), paving a route towards the generation of long-range and robust entanglement of photons [96]. Similarly, in an N -level emitter multi-photon bound states can be made to destructively interfere with the standard multi-photon transmission, effectively suppressing multi-photon transmission and leading to a photonic blockade without the need for a cavity [75].

IV. NONLINEAR RESPONSE OF COUPLED MULTI-EMITTER SYSTEMS

One of the most difficult and potentially most rewarding challenges in modern quantum optics is the scaling of individual elements into more complex quantum systems. Both aspects, the difficulty and the reward, are reflected in recent works on multi-emitter waveguide QED, the vast majority of which are theoretical in nature. Practically, the task is that the emitters of such a system simultaneously fulfill the following requirements: (i) They must all couple to the same guided mode, and in general this coupling should be efficient. (ii) The emitters should all interact coherently with passing photons (i.e. $\Gamma_{\text{deph}} \approx 0$, c.f. Sec. II A). (iii) The emitters should emit at a similar transition frequency and have similar linewidths. (iv) Ideally, the emitters could be individually addressed such that their relative coupling can be controlled (e.g. by local electrical gating).

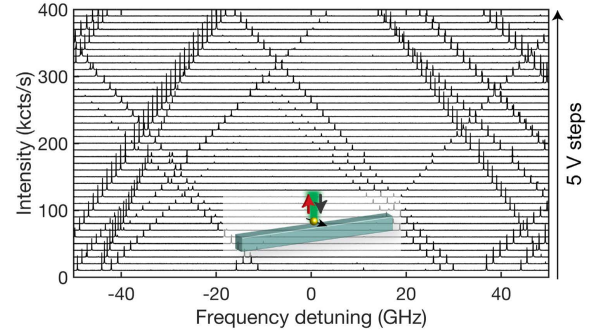
As we outlined in Sec. II conditions (i) and (ii) have been met for a single emitter coupled to a waveguide, and the current experimental challenges lie in meeting criteria (iii) and (iv). First efforts in this direction involved the entanglement of two implanted Si-vacancy defects coupled to a single waveguide, first using a remote Raman control scheme [24] and then directly via strain tuning [107]. A signature of the entanglement between the two emitters was observed in their photon correlations. Similarly, superradiance has been observed using ensembles with a mean number of atoms ≤ 6 coupled to waveguide [31, 66], although here the emitters could not be individually addressed. In contrast, micro-electrodes were shown to Stark-shift the resonance of many individual molecules coupled to a nanoguide [105, 108] (see **Fig. 7a**). These experiments demonstrate that an efficient and controllable coupling of multiple solid-state emitters on a photonic chip is within reach [109].

Coupling quantum emitters with waveguides has been the focus of intense theoretical studies in recent years, resulting in prediction of both emergent many-body phenomena and new protocols for quantum information technology. This is already exemplified in two-emitter systems that, even when coupled to a lossy waveguide, can result in sub- and super-radiant states, allow for two-qubit gates [110] and entanglement generation [111, 112]. Conversely, the high efficiency with which individual solid-state emitters can couple to a waveguide allows for the entanglement and coupling of qubits that operate at vastly different frequencies, such as superconducting qubits with single molecules [113] or quantum dots [114]. Similarly, the input-output formalism was used to study quantum interference and photon statistics in a two-qubit system, demonstrating the complex dynamics that result from the quantum jumps of the emitters [115].

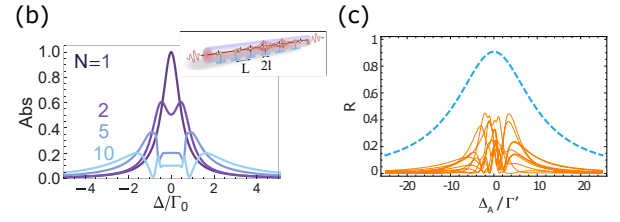
Concurrently, frameworks describing photonic transport through waveguides coupled to many emitters have been developed. Models focusing on specific aspects of this transport have quantified both the photon-

Nonlinear response of coupled multi emitters

(a) Stark Tuning of multiple emitters



Multiple emitters systems



(d) Optical switching of photons

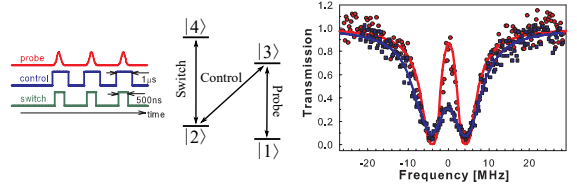


FIG. 7. (a) Stark tuning of many organic molecules found within a single confocal excitation spot, as shown in the inset. Spectra taken at different Stark voltages demonstrate that it is possible to tune multiple emitters into resonance with one another on a photonic chip. Adapted from [105]. (b) Absorption spectrum calculated for a chain of well-coupled N emitters ($\beta = 0.99$) arranged at arbitrary positions about a regular lattice spacing $L = 2.75$ in a nanoguide (see inset). As the number of emitters increases (dark to light hues), normal-mode splitting is observed, while for $N = 10$ narrow peaks near zero detuning $\Delta = 0$ emerge due to the presence of sub-radiant modes. Adapted from [50]. (c) Reflection spectra for 20 atoms interacting through the guided modes of an unstructured waveguide. The dashed blue line represents a regular separation between the atoms of $\lambda/2$. The orange curves show 10 different spectra obtained by randomly placing the atoms along the nanostructure. Adapted from [51]. (d) Nonlinear optical switch based on four-level emitters coupled to a fiber. The timing sequence for the probe, control and switch fields (right) and the corresponding level scheme of the emitters (center). Left: In the absence of the switch field, the probe field is largely transmitted through the fiber (red data). A strong suppression of the transmission is observed when the switch field is on (blue data). Adapted from [106].

photon [116] and emitter-emitter [117] entanglement that is generated as photons interact with the emitters, showing that this entanglement is more robust and efficient in chiral geometries. Interestingly, researchers have predicted that stronger photonic correlations lead to lower propagation losses, even if the emitters are weakly coupled to the waveguide or in the presence of disorder [118]. Similarly, efficient multiple scattering events between the emitters have been predicted to allow for normal mode-splitting without the need for cavities, and for the emergence of localized excitations [50] (c.f. Fig. 7a) and ‘fermionic’ subradiant modes that repel one another [119].

Many different effects and geometries of one-dimensional, multi-emitter systems have been modelled. These include the addition of evanescent emitter-emitter coupling for closely spaced emitters [50, 120] and the inclusion of different decoherence mechanisms and inhomogeneous broadening [94]. Likewise, Pivovarov *et al.*, developed a general microscopic model to describe single-photon scattering from a chain of multi-level emitters that describes both ordered and disordered geometries, and including both elastic and inelastic scattering channels [121]. Das *et al.*, meanwhile, modeled the dynamics and amplitudes of the scattering of photons from multi-level emitters in the low excitation limit, working in the Heisenberg picture [122]. In this same, low-excitation regime ($\langle \hat{\sigma}_{ee} \rangle = 0$), the Green’s tensor approach outlined in Sec. II was generalized to N -emitters [51]. For two level emitters, in this Green’s function formalism, the generalized equation of motion for the emitter coherences is

$$\dot{\hat{\sigma}}_{ge}^i = i \left(\Delta_A + i \frac{\Gamma'}{2} \right) \hat{\sigma}_{ge}^i + i \Omega^i + i \sum_j g_{ij} \hat{\sigma}_{ge}^j, \quad (16)$$

where zero dephasing is also assumed. Here, the superscripts i and j refer to specific emitters, Γ' is the rate of emission into the non-guided modes, and g_{ij} is the dipole projected Green’s function as defined in Eq. 7. Note, however, that in this case g_{ij} controls the interactions between the emitters, which can be either dispersive or dissipative, depending on whether the real or imaginary component of $\mathbf{G}(\mathbf{r}_i, \mathbf{r}_j)$ dominates. The general nature of this approach means that it can be applied to a variety of nanophotonic structures, including emitter chains

in unstructured waveguides, cavities and photonic crystals, as was done in [51] (Fig. 7b). Protocols, based on these theories, have begun to emerge, including schemes for quantum computation [6] and the efficient generation of multiphoton states [123].

The large nonlinearity inherent to quantum emitters manifests in novel fashion when many multilevel emitters are coupled via waveguides. Emitters in the EIT configuration, for example, can exhibit a giant Kerr nonlinearity [124]. Using a hollow-core photonic crystal fiber as a waveguide, to which they coupled a large ensemble of Rydberg atoms, researchers were able to exploit this Kerr nonlinearity for few-photon switching [106] (Fig. 7c). A recent theoretical treatment of this system predicts that, in the ideal case, single-photon switching is possible and studies the nonlinear evolution of two-photon wavepacket (c.f. Sec. IIB) [125]. Photons travelling through such a multi-emitter system have also been predicted to crystalize, forming fermionic excitations that repel one another and providing an additional route to the creation of a pure, single-photon source and enabling the study of complex quantum phase transitions [126]. Interestingly, the long-range interactions in such multi-emitter-waveguide systems are expected to give rise to nonlocal optical nonlinearities [127], providing yet another route to the creation of photonic bound-states [128].

V. CONCLUSIONS AND OUTLOOK

Advances in the growth and preparation of solid-state emitters and nanofabrication protocols have, in recent years, brought coherent light-matter interactions to quantum photonic chips. For single-emitter systems, these advances have allowed for the observation of a variety of nonlinear optical effects at, or near, the single-photon level, bringing a host of classical and quantum functionalities tantalizingly within reach. At the same time, increasingly complex theories have been developed that model the coupling of multiple emitters via long-range, waveguide-mediated interactions. Such multi-emitter systems have been predicted to support exotic new quantum phases of light and may enable efficient new quantum information technologies. Experimentally, we stand at the cusp of this exciting field, with multi-emitter photonic architectures just around the corner.

-
- [1] C. Noh and D. G. Angelakis, Rep. Prog. Phys. **80**, 016401 (2017).
 - [2] H. J. Kimble, Nature **453**, 1023 (2008).
 - [3] S. Ritter, C. Nölleke, C. Hahn, A. Reiserer, A. Neuzner, M. Uphoff, M. Mücke, E. Figueroa, J. Bochmann, and G. Rempe, Nature **484**, 195 (2012).
 - [4] P. Lodahl, Quant. Sci. Tech. **3**, 013001 (2018).
 - [5] D. P. DiVincenzo, D. Bacon, J. Kempe, G. Burkard, and K. B. Whaley, Nature **408**, 339 (2000).
 - [6] V. Paulisch, H. J. Kimble, and A. González-Tudela, New J. Phys. **18**, 043041 (2016).
 - [7] D. E. Chang, A. S. Sørensen, P. R. Hemmer, and M. D. Lukin, Phys. Rev. Lett. **97**, 053002 (2006).
 - [8] I. Friedler, C. Sauvan, J. P. Hugonin, P. Lalanne, J. Claudon, and J. M. Gérard, Opt. Express **17**, 2095 (2009).
 - [9] P. Lodahl, S. Mahmoodian, and S. Stobbe, Rev. Mod. Phys. **87**, 347 (2015).

- [10] Q. Wang, S. Stobbe, and P. Lodahl, *Phys. Rev. Lett.* **107**, 167404 (2011).
- [11] M. Arcari, I. Söllner, A. Javadi, S. Lindskov Hansen, S. Mahmoodian, J. Liu, H. Thyrestrup, E. H. Lee, J. D. Song, S. Stobbe, and P. Lodahl, *Phys. Rev. Lett.* **113**, 093603 (2014).
- [12] G. Kiršanskė, H. Thyrestrup, R. S. Daveau, C. L. Dreessen, T. Pregnolato, L. Midolo, P. Tighineanu, A. Javadi, S. Stobbe, R. Schott, A. Ludwig, A. D. Wieck, S. I. Park, J. D. Song, A. V. Kuhlmann, I. Söllner, M. C. Löbl, R. J. Warburton, and P. Lodahl, *Phys. Rev. B* **96**, 165306 (2017).
- [13] J. Carolan, C. Harrold, C. Sparrow, E. Martín-López, N. J. Russell, J. W. Silverstone, P. J. Shadbolt, N. Matsuda, M. Oguma, M. Itoh, G. D. Marshall, M. G. Thompson, J. C. F. Matthews, T. Hashimoto, J. L. O'Brien, and A. Laing, *Science* **349**, 711 (2015).
- [14] J. Wang, S. Paesani, Y. Ding, R. Santagati, P. Skrzypczyk, A. Salavrakos, J. Tura, R. Augusiak, L. Mančinska, D. Bacco, D. Bonneau, J. W. Silverstone, Q. Gong, A. Acín, K. Rottwitt, L. K. Oxenløwe, J. L. O'Brien, A. Laing, and M. G. Thompson, *Science* **360**, 285 (2018).
- [15] J. Petersen, J. Volz, and A. Rauschenbeutel, *Science* **346**, 67 (2014).
- [16] B. le Feber, N. Rotenberg, and L. Kuipers, *Nature Commun.* **6**, 6695 (2015).
- [17] I. Söllner, S. Mahmoodian, S. L. Hansen, L. Midolo, A. Javadi, G. Kiršanskė, T. Pregnolato, H. El-Ella, E. H. Lee, J. D. Song, S. Stobbe, and P. Lodahl, *Nature Nanotech.* **10**, 775 (2015).
- [18] R. J. Coles, D. M. Price, J. E. Dixon, B. Royall, E. Clarke, P. Kok, M. S. Skolnick, A. M. Fox, and M. N. Makhonin, *Nature Commun.* **7**, 11183 (2016).
- [19] P. Lodahl, S. Mahmoodian, S. Stobbe, A. Rauschenbeutel, P. Schneeweiss, J. Volz, H. Pichler, and P. Zoller, *Nature* **541**, 473 (2017).
- [20] S. Faez, P. Türschmann, H. R. Haakh, S. Götzinger, and V. Sandoghdar, *Phys. Rev. Lett.* **113**, 213601 (2014).
- [21] P. Türschmann, N. Rotenberg, J. Renger, O. Harder, I. Lohse, T. Utikal, S. Götzinger, and V. Sandoghdar, *Nano Lett.* **17**, 4941 (2017).
- [22] P. Lombardi, A. P. O'vvy, S. Pazzagli, G. Mazzamuto, G. Kewes, O. Neitzke, N. Gruhler, O. Benson, W. H. P. Pernice, F. S. Cataliotti, and C. Toninelli, *ACS Photon.* **5**, 126 (2017).
- [23] S. M. Skoff, D. Papencordt, H. Schauffert, B. C. Bayer, and A. Rauschenbeutel, *Phys. Rev. A* **97**, 043839 (2018).
- [24] A. Sipahigil, R. E. Evans, D. D. Sukachev, M. J. Burek, J. Borregaard, M. K. Bhaskar, C. T. Nguyen, J. L. Pacheco, H. A. Atikian, C. Meuwly, R. M. Camacho, F. Jelezko, E. Bielejec, H. Park, M. Lončar, and M. D. Lukin, *Science* **354**, 847 (2016).
- [25] M. Schukraft, J. Zheng, T. Schröder, S. L. Mouradian, M. Walsh, M. E. Trusheim, H. Bakhru, and D. R. Englund, *APL Photonics* **1**, 020801 (2016).
- [26] M. K. Bhaskar, D. Sukachev, A. Sipahigil, R. Evans, M. Burek, C. Nguyen, L. Rogers, P. Siyushev, M. Metsch, H. Park, F. Jelezko, M. Lončar, and M. Lukin, *Phys. Rev. Lett.* **118**, 223603 (2017).
- [27] M. J. Burek, C. Meuwly, R. E. Evans, M. K. Bhaskar, A. Sipahigil, S. Meesala, B. Machielse, D. D. Sukachev, C. T. Nguyen, J. L. Pacheco, E. Bielejec, M. D. Lukin, and M. Lončar, *Phys. Rev. Appl.* **8**, 024026 (2017).
- [28] E. Vetsch, D. Reitz, G. Sagué, R. Schmidt, S. T. Dawkins, and A. Rauschenbeutel, *Phys. Rev. Lett.* **104**, 203603 (2010).
- [29] A. Goban, K. S. Choi, D. J. Alton, D. Ding, C. Lacroûte, M. Pototschnig, T. Thiele, N. P. Stern, and H. J. Kimble, *Phys. Rev. Lett.* **109**, 033603 (2012).
- [30] R. Mitsch, C. Sayrin, B. Albrecht, P. Schneeweiss, and A. Rauschenbeutel, *Nat. Commun.* **5**, 5713 (2014).
- [31] J. D. Hood, A. Goban, A. Asenjo-Garcia, M. Lu, S.-P. Yu, D. E. Chang, and H. J. Kimble, *Proc. Nat. Acad. Sci.* **113**, 10507 (2016).
- [32] D. Roy, C. M. Wilson, and O. Firstenberg, *Rev. Mod. Phys.* **89**, 021001 (2017).
- [33] A. V. Kuhlmann, J. Houel, A. Ludwig, L. Greuter, D. Reuter, A. D. Wieck, M. Poggio, and R. J. Warburton, *Nature Phys.* **9**, 570 (2013).
- [34] A. Thoma, P. Schnauber, M. Gschrey, M. Seifried, J. Wolters, J.-H. Schulze, A. Strittmatter, S. Rodt, A. Carmele, A. Knorr, T. Heindel, and S. Reitzenstein, *Phys. Rev. Lett.* **116**, 033601 (2016).
- [35] S. Grandi, K. D. Major, C. Polisseni, S. Boissier, A. S. Clark, and E. A. Hinds, *Phys. Rev. A* **94**, 063839 (2016).
- [36] P. Tighineanu, C. L. Dreeßen, C. Flindt, P. Lodahl, and A. S. Sørensen, *Phys. Rev. Lett.* **120**, 257401 (2018).
- [37] B. Gmeiner, A. Maser, T. Utikal, S. Götzinger, and V. Sandoghdar, *Phys. Chem. Chem. Phys.* **18**, 19588 (2016).
- [38] N. Somaschi, V. Giesz, L. De Santis, J. C. Lored, M. P. Almeida, G. Hornecker, S. L. Portalupi, T. Grange, C. Antn, J. Demory, C. Gmez, I. Sagnes, N. D. Lanzillotti-Kimura, A. Lematre, A. Auffeves, A. G. White, L. Lanco, and P. Senellart, *Nature Photon.* **10**, 340 (2016).
- [39] M. C. Löbl, I. Söllner, A. Javadi, T. Pregnolato, R. Schott, L. Midolo, A. V. Kuhlmann, S. Stobbe, A. D. Wieck, P. Lodahl, A. Ludwig, and R. J. Warburton, *Phys. Rev. B* **96**, 165440 (2017).
- [40] X. Ding, Y. He, Z.-C. Duan, N. Gregersen, M.-C. Chen, S. Unsleber, S. Maier, C. Schneider, M. Kamp, S. Höfling, C.-Y. Lu, and J.-W. Pan, *Phys. Rev. Lett.* **116**, 020401 (2016).
- [41] D. Rattenbacher, A. Shkarin, J. Renger, T. Utikal, S. Götzinger, and V. Sandoghdar, *arXiv:1902.05257* (2019).
- [42] B. C. Rose, D. Huang, Z.-H. Zhang, P. Stevenson, A. M. Tyryshkin, S. Sangtawesin, S. Srinivasan, L. Loudin, M. L. Markham, A. M. Edmonds, D. J. Twitchen, S. A. Lyon, and N. P. de Leon, *Science* **361**, 60 (2018).
- [43] Z. Liao, X. Zeng, H. Nha, and M. S. Zubairy, *Phys. Scr.* **91**, 063004 (2016).
- [44] W. Vogel and D.-G. Welsch, *Quantum Optics*, 3rd ed. (Wiley-VCH, 2006).
- [45] P. Meystre and M. Sargent, *Elements of Quantum Optics* (Springer, 2007).
- [46] H. T. Dung, L. Knöll, and D.-G. Welsch, *Phys. Rev. A* **66**, 063810 (2002).
- [47] Z. Ficek and R. Tanas, *Phys. Rep.* **372**, 369 (2002).
- [48] T. Gruner and D.-G. Welsch, *Phys. Rev. A* **53**, 1818 (1996).
- [49] S. Y. Buhmann, *Dispersion Forces I* (Springer, 2012).

- [50] H. R. Haakh, S. Faez, and V. Sandoghdar, *Phys. Rev. A* **94**, 053840 (2016).
- [51] A. Asenjo-Garcia, J. D. Hood, D. E. Chang, and H. J. Kimble, *Phys. Rev. A* **95**, 033818 (2017).
- [52] H. Thyrestrup, G. Kiršanskė, H. Le Jeannic, T. Pregnolato, L. Zhai, L. Raahauge, L. Midolo, N. Rotenberg, A. Javadi, R. Schott, A. D. Wieck, A. Ludwig, M. C. Löbl, I. Söllner, R. J. Warburton, and P. Lodahl, *Nano Lett.* **18**, 1801 (2018).
- [53] I. Gerhardt, G. Wrigge, P. Bushev, G. Zumofen, M. Agio, R. Pfab, and V. Sandoghdar, *Phys. Rev. Lett.* **98**, 033601 (2007).
- [54] G. Zumofen, N. M. Mojarad, V. Sandoghdar, and M. Agio, *Phys. Rev. Lett.* **101**, 180404 (2008).
- [55] Private communication with H.R. Haakh..
- [56] T. G. Tiecke, J. D. Thompson, N. P. de Leon, L. R. Liu, V. Vuletić, and M. D. Lukin, *Nature* **508**, 241 (2014).
- [57] A. Auffèves-Garnier, C. Simon, J.-M. Gérard, and J.-P. Poizat, *Phys. Rev. A* **75**, 053823 (2007).
- [58] D. Wang, H. Kelkar, D. Martin-Cano, D. Rattenbacher, A. Shkarin, T. Utikal, S. Götzinger, and V. Sandoghdar, *Nature Phys.* (2019).
- [59] R. E. Evans, M. K. Bhaskar, D. D. Sukachev, C. T. Nguyen, A. Sipahigil, M. J. Burek, B. Machiels, G. H. Zhang, A. S. Zibrov, E. Bielejec, H. Park, M. Lončar, and M. D. Lukin, *Science* **362**, 662 (2018).
- [60] D. Najer, I. Söllner, P. Sekatski, V. Dolique, M. C. Löbl, D. Riedel, R. Schott, S. Starosielec, S. R. Valentin, A. D. Wieck, N. Sangouard, A. Ludwig, and R. J. Warburton, *arXiv:1812.08662v1* (2018).
- [61] A. Javadi, I. Söllner, M. Arcari, S. Lindskov Hansen, L. Midolo, S. Mahmoodian, G. Kiršanskė, T. Pregnolato, E. Lee, J. Song, S. Stobbe, and P. Lodahl, *Nature Commun.* **6**, 8655 (2015).
- [62] D. Hallett, A. P. Foster, D. L. Hurst, B. Royall, P. Kok, E. Clarke, I. E. Itskevich, A. M. Fox, M. S. Skolnick, and L. R. Wilson, *Optica* **5**, 644 (2018).
- [63] H. le Jeannic and *et. al.*, In Preparation.
- [64] H. Snijders, J. A. Frey, J. Norman, M. P. Bakker, E. C. Langman, A. Gossard, J. E. Bowers, M. P. van Exter, D. Bouwmeester, and W. Löffler, *Nature Commun.* **7**, 12578 (2016).
- [65] N. V. Corzo, J. Raskp, A. Chandra, A. S. Sheremet, B. Gouraud, and J. Laurat, *Nature* **566**, 359 (2019).
- [66] P. Solano, P. Barberis-Blostein, F. K. Fatemi, L. A. Orozco, and S. L. Rolston, *Nature Commun.* **8**, 1857 (2017).
- [67] D. Chang, A. Sørensen, E. Demler, and M. Lukin, *Nature Phys.* **3**, 807 (2007).
- [68] J.-T. Shen and S. Fan, *Phys. Rev. Lett.* **98**, 153003 (2007).
- [69] J.-T. Shen and S. Fan, *Phys. Rev. A* **76**, 062709 (2007).
- [70] S. Fan, S. E. Kocabaş, and J.-T. Shen, *Phys. Rev. A* **82**, 063821 (2010).
- [71] T. Ramos and J. J. García-Ripoll, *Phys. Rev. Lett.* **119**, 153601 (2017).
- [72] P. Longo, P. Schmitteckert, and K. Busch, *Phys. Rev. Lett.* **104**, 023602 (2010).
- [73] P. Longo, P. Schmitteckert, and K. Busch, *Phys. Rev. A* **83**, 063828 (2011).
- [74] P. Törmä and W. L. Barnes, *Rep. Prog. Phys.* **78**, 013901 (2014).
- [75] H. Zheng, D. J. Gauthier, and H. U. Baranger, *Phys. Rev. A* **82**, 063816 (2010).
- [76] E. Sánchez-Burillo, D. Zueco, L. Martín-Moreno, and J. J. García-Ripoll, *Phys. Rev. A* **96**, 023831 (2017).
- [77] O. Firstenberg, T. Peyronel, Q.-Y. Liang, A. V. Gorshkov, M. D. Lukin, and V. Vuletić, *Nature* **502**, 71 (2013).
- [78] Q.-Y. Liang, A. V. Venkatramani, S. H. Cantu, T. L. Nicholson, M. J. Gullans, A. V. Gorshkov, J. D. Thompson, C. Chin, M. D. Lukin, and V. Vuletić, *Science* **359**, 783 (2018).
- [79] N. Stiesdal, J. Kumlin, K. Kleinbeck, P. Lunt, C. Braun, A. Paris-Mandoki, C. Tresp, H. P. Büchler, and S. Hofferberth, *Phys. Rev. Lett.* **121**, 103601 (2018).
- [80] D. Witthaut, M. D. Lukin, and A. S. Sørensen, *EPL (Europhysics Letters)* **97**, 50007 (2012).
- [81] T. C. Ralph, I. Söllner, S. Mahmoodian, A. White, and P. Lodahl, *Phys. Rev. Lett.* **114**, 173603 (2015).
- [82] D. Roy, *Phys. Rev. B* **81**, 155117 (2010).
- [83] F. Y. Wu, S. Ezekiel, M. Ducloy, and B. R. Mollow, *Phys. Rev. Lett.* **38**, 1077 (1977).
- [84] A. Maser, B. Gmeiner, T. Utikal, S. Götzinger, and V. Sandoghdar, *Nature Photon.* **10**, 450 (2016).
- [85] A. Lezama, Y. Zhu, M. Kanskär, and T. W. Mossberg, *Phys. Rev. A* **41**, 1576 (1990).
- [86] S. Papademetriou, S. Chakmakjian, and C. R. Stroud, *J. Opt. Soc. Am. B* **9**, 1182 (1992).
- [87] F. Jelezko, B. Lounis, and M. Orrit, *J. Chem. Phys.* **107**, 1692 (1997).
- [88] X. Xu, B. Sun, P. R. Berman, D. G. Steel, A. S. Bracker, D. Gammon, and L. J. Sham, *Science* **317**, 929 (2007).
- [89] X. Xu, B. Sun, E. D. Kim, K. Smirl, P. R. Berman, D. G. Steel, A. S. Bracker, D. Gammon, and L. J. Sham, *Phys. Rev. Lett.* **101**, 227401 (2008).
- [90] M. Fleischhauer, A. Imamoglu, and J. P. Marangos, *Rev. Mod. Phys.* **77**, 633 (2005).
- [91] T. Chanelièr, D. N. Matsukevich, S. D. Jenkins, S.-Y. Lan, T. A. B. Kennedy, and A. Kuzmich, *Nature* **483**, 833 (2005).
- [92] C. Sayrin, C. Clausen, B. Albrecht, P. Schneeweiss, and A. Rauschenbeutel, *Optica* **2**, 353 (2015).
- [93] F. Le Kien and A. Rauschenbeutel, *Phys. Rev. A* **91**, 053847 (2015).
- [94] G.-Z. Song, E. Munro, W. Nie, F.-G. Deng, G.-J. Yang, and L.-C. Kwek, *Phys. Rev. A* **96**, 043872 (2017).
- [95] D. Witthaut and A. S. Srensen, *New J. Phys.* **12**, 043052 (2010).
- [96] D. Roy, *Phys. Rev. Lett.* **106**, 053601 (2011).
- [97] P. Bermel, A. Rodriguez, S. G. Johnson, J. D. Joannopoulos, and M. Soljačić, *Phys. Rev. A* **74**, 043818 (2006).
- [98] S. Xu and S. Fan, *APL Photonics* **3**, 116102 (2018).
- [99] J. Hwang, M. Pototschnig, R. Lettow, G. Zumofen, A. Renn, S. Götzinger, and V. Sandoghdar, *Nature* **460**, 76 (2009).
- [100] G. Kewes, M. Schoengen, O. Neitzke, P. Lombardi, R.-S. Schönfeld, G. Mazzamuto, A. W. Schell, J. Probst, J. Wolters, B. Löchel, C. Toninelli, and O. Benson, *Sci. Rep.* **6**, 28877 (2016).
- [101] P. Kolchin, R. F. Oulton, and X. Zhang, *Phys. Rev. Lett.* **106**, 113601 (2011).
- [102] T. Y. Li, J. F. Huang, and C. K. Law, *Phys. Rev. A* **91**, 043834 (2015).
- [103] R. Raussendorf and H. J. Briegel, *Phys. Rev. Lett.* **86**, 5188 (2001).

- [104] H. Zheng, D. J. Gauthier, and H. U. Baranger, Phys. Rev. A **85**, 043832 (2012).
- [105] P. Türschmann, N. Rotenberg, J. Renger, O. Harder, I. Lohse, T. Utikal, S. Götzinger, and V. Sandoghdar, arXiv:1702.05923 (2017).
- [106] M. Bajcsy, S. Hofferberth, V. Balic, T. Peyronel, M. Hafezi, A. S. Zibrov, V. Vuletic, and M. D. Lukin, Phys. Rev. Lett. **102**, 203902 (2009).
- [107] B. Machielse, S. Bogdanovic, S. Meesala, S. Gauthier, M. J. Burek, G. Joe, M. Chalupnik, Y.-K. Sohn, J. Holzgrafe, R. E. Evans, C. Chia, H. Atikian, M. K. Bhaskar, D. D. Sukachev, L. Shao, S. Maity, M. D. Lukin, and M. Lončar, arXiv:1901.09103 (2019).
- [108] P. Türschmann, *Coherent Coupling of Organic Dye Molecules to Optical Nanoguides* (FAU University Press, 2018).
- [109] P. Lodahl, Science **362**, 646 (2018).
- [110] D. Dzsofjan, A. S. Sørensen, and M. Fleischhauer, Phys. Rev. B **82**, 075427 (2010).
- [111] A. Gonzalez-Tudela, D. Martin-Cano, E. Moreno, L. Martin-Moreno, C. Tejedor, and F. J. Garcia-Vidal, Phys. Rev. Lett. **106**, 020501 (2011).
- [112] D. Martín-Cano, A. González-Tudela, L. Martín-Moreno, F. J. García-Vidal, C. Tejedor, and E. Moreno, Phys. Rev. B **84**, 235306 (2011).
- [113] S. Das, V. E. Elfving, S. Faez, and A. S. Sørensen, Phys. Rev. Lett. **118**, 140501 (2017).
- [114] V. E. Elfving, S. Das, and A. S. Sørensen, arXiv:1810.01381 (2018).
- [115] X. H. H. Zhang and H. U. Baranger, Phys. Rev. A **97**, 023813 (2018).
- [116] Y.-L. L. Fang and H. U. Baranger, Phys. Rev. A **91**, 053845 (2015).
- [117] I. M. Mirza and J. C. Schotland, Phys. Rev. A **94**, 012302 (2016).
- [118] S. Mahmoodian, M. Čepulkovskis, S. Das, P. Lodahl, K. Hammerer, and A. S. Sørensen, Phys. Rev. Lett. **121**, 143601 (2018).
- [119] A. Albrecht, L. Henriët, A. Asenjo-Garcia, P. B. Dieterle, O. Painter, and D. E. Chang, arXiv:1803.02115 (2018).
- [120] M.-T. Cheng, J. Xu, and G. S. Agarwal, Phys. Rev. A **95**, 053807 (2017).
- [121] V. A. Pivovarov, A. S. Sheremet, L. V. Gerasimov, V. M. Porozova, N. V. Corzo, J. Laurat, and D. V. Kupriyanov, Phys. Rev. A **97**, 023827 (2018).
- [122] S. Das, V. E. Elfving, F. Reiter, and A. S. Sørensen, Phys. Rev. A **97**, 043838 (2018).
- [123] A. González-Tudela, V. Paulisch, H. J. Kimble, and J. I. Cirac, Phys. Rev. Lett. **118**, 213601 (2017).
- [124] H. Schmidt and A. Imamoglu, Opt. Lett. **21**, 1936 (1996).
- [125] M. Hafezi, D. E. Chang, V. Gritsev, E. Demler, and M. D. Lukin, Phys. Rev. A **85**, 013822 (2012).
- [126] D. E. Chang, V. Gritsev, G. Morigi, V. Vuletić, M. D. Lukin, and E. A. Demler, Nature Phys. **4**, 884 (2008).
- [127] E. Shahmoon, P. Grišins, H. P. Stimming, I. Mazets, and G. Kurizki, Optica **3**, 725 (2016).
- [128] J. S. Douglas, T. Caneva, and D. E. Chang, Phys. Rev. X **6**, 031017 (2016).